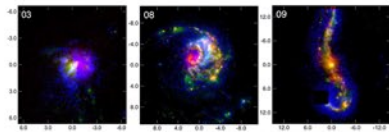


Introduction

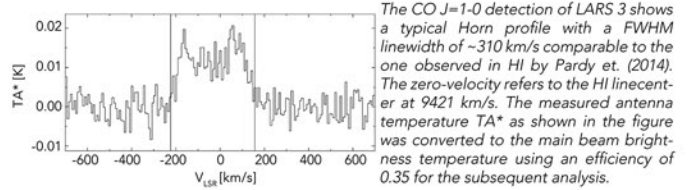
Lyman Alpha emission plays a crucial role for observations of the high-redshift Universe since recombination nebulae reprocess approximately 1/3 of the raw ionizing power into a single emission line. Therefore, many thousands of high-z galaxies were observed and studied using the Lyman Alpha line to date. However, its interpretation is complex, because of resonant scattering of Lyman photons. The only way to remedy this complicated situation is to study the Lyman Alpha emission on a spatially resolved basis in a local sample of galaxies such as our Lyman Alpha Reference Sample (LARS; Hayes et al. 2013, 2014). LARS counts 14 galaxies, is statistically meaningful enough to observe trends and, most importantly, comparable in selection to galaxies observed at high-z (e.g. Ouchi et al 2008; Cowie et al 2011). Beside the importance of Lyman Alpha analysis for gaining insight into the early Universe, Carbon Monoxide (^{12}CO) transitions are increasingly observed at high-z. Although sample sizes are still small, the cosmic evolution of star formation efficiency (SFE), relies on ^{12}CO observations. Recent studies find evidence for an increase in SFE with redshift, but caution that the results are most sensitive to the applied conversion factor, which ultimately defines the molecular gas fraction.



False-color images of three LARS galaxies. Red encodes continuum subtracted Ha, Green the FUV continuum and blue shows continuum subtracted Ly α . The black square in LARS 09 masks a UV-bright field star. Scales in kiloparsec are given on the side.

^{12}CO Observations

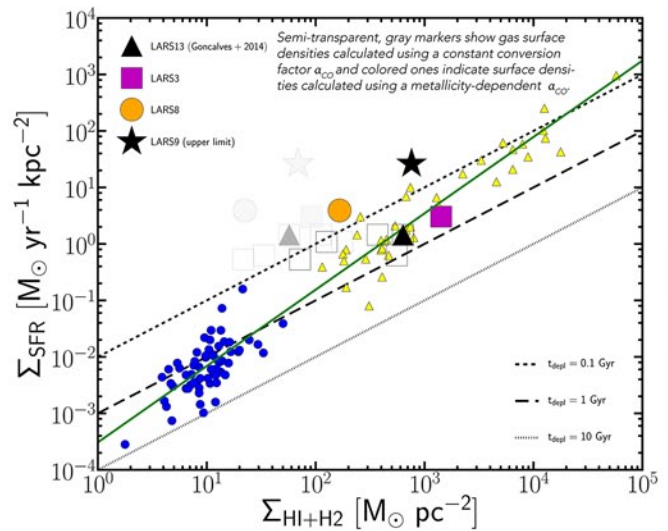
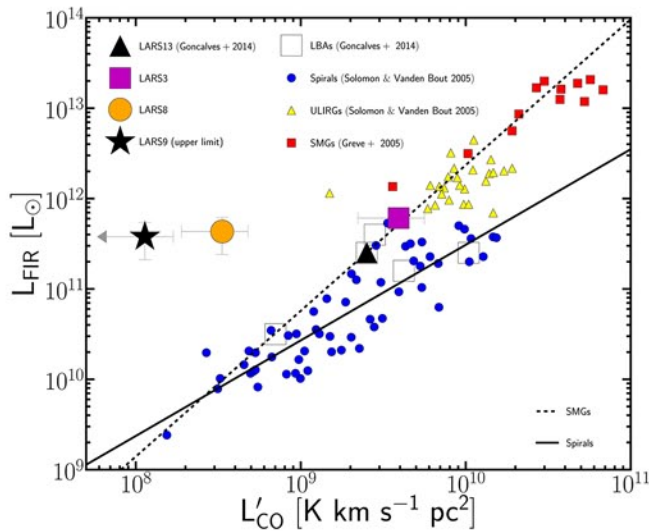
We observed three LARS (3, 8, 9) galaxies at $z \sim 0.04$ in the $^{12}\text{CO} J=1-0$ line during May 2014 using the 45m telescope at the Nobeyama Radio Observatory (NRO). The beamsize at 115 GHz is $\sim 15''$ corresponding to ~ 12 kpc at the given redshift. The T21 and T22 receivers were used simultaneously in dual-beam mode with one of the beams always on-source and the SAM45 spectrometer was used as a backend. The system-noise temperature T_{sys} was typically 220 K during our observations. The telescope pointing was checked every hour by observing a SiO maser source at 43 GHz. Only data with a pointing accuracy better than $5''$ was used for the analysis. We detected strong ^{12}CO emission in LARS 3, marginally detected LARS 8 and derived an upper limit for LARS 9. Our data reduction was done using the NEWSTAR software, which was developed by NRO based on the Astronomical Image Processing System (AIPS) package.



The CO $J=1-0$ detection of LARS 3 shows a typical Horn profile with a FWHM linewidth of ~ 310 km/s comparable to the one observed in HI by Pardy et. (2014). The zero-velocity refers to the HI linecenter at 9421 km/s. The measured antenna temperature T_A^* as shown in the figure was converted to the main beam brightness temperature using an efficiency of 0.35 for the subsequent analysis.

Analysis and Results

We present and discuss the CO/IR relation (left figure) and the unresolved Kennicutt-Schmidt (KS) law (right figure) for LARS galaxies. In both cases we include archival ^{12}CO data of LARS 13 published by Gonçalves et al. (2014). The fluxes were first converted into ^{12}CO luminosities according to a standard cosmology with $H_0=70$, $\Omega_M=0.3$ and $\Omega_{\text{vac}}=0.7$. The luminosities were then corrected for aperture effects - the coupling between a Gaussian beam with an assumed exponential ^{12}CO distribution with a scale length of $0.23 D_{25}$ with D_{25} the diameter in the optical B-band at which the surface brightness declines to 25 mag/arcsec 2 . The CO/IR relation reveals that LARS 8 and 9 are far off the location of local spirals or ULIRGs, whereas LARS 3 and LARS 13 do fall into the ULIRG region. The offset can partly be explained by low/intermediate metallicity effects leading to large CO to H_2 conversion factors α_{CO} . This is supported by the fact that LARS 9, for which only an upper limit could be calculated, the metallicity indeed is lowest in the present CO subsample with $[12+\log(\text{O}/\text{H})]=8.36$. Additionally, we find that a constant Milky Way conversion factor finally leads to a huge scatter in the KS law, whereas with a metallicity-dependent α_{CO} the scatter becomes much smaller. However, even after accounting for metallicity effects by calculating α_{CO} using empirical findings of Magdis+ (2011) which is based on the gas-to-dust-ratio vs. metallicity relation, our observations suggest that the SFE in our sample is dramatically increased by a factor up to ~ 10 compared to normal spirals, which affirms the suitability of LARS as a proxy for high-redshift galaxies, because such a behaviour is commonly observed at high-z. We interpret the enhanced SFE as a result of shock heating in the ISM introduced by tidal forces. Subsequently, the external ISM pressure exceeding the dynamical pressure of molecular clouds, supports their collapse and triggers fragmentation. As shown by Zubovas et al. (2014), in such environments of high pressure, new stars preferable form in massive and compact clusters located in the centre of the initial cloud rather than along cloud filaments. This is supported by our HST images which reveal tidal features as a result of merging processes and the existence of dense and supermassive stellar associations. Additionally, at least for LARS 9, this scenario is upheld by our Herschel/PACS spectroscopy, because the observed [CII] 158 μm line is too strong to be explained by cooling in photo-dissociation regions (PDRs) from star formation only. Most likely, the galaxy contains large amounts of shock-heated gas undergoing turbulent energy dissipation.



References

Combes (2014), "Cosmic evolution of gas content and accretion", arXiv:1405.6405, to be published in Seychelles conference on galaxy evolution "Lessons from the Local Group", ed. Freeman+, 2014
 Cowie+ (2011), "Ly α Emitting Galaxies as Early Stages in Galaxy Formation", APJ, Volume 738, Issue 2, id. 136, 22 pp., 2011
 Freundlich+ (2013), "Towards a resolved Kennicutt-Schmidt law at high redshift", A&A, Volume 553, id. A130, 6 pp., 2013
 Gonçalves+ (2014), "Molecular gas properties of UV-bright star-forming galaxies at low redshift", MNRAS, Volume 442, Issue 2, p. 1429-1439, 2014
 Hayes+ (2014), "Lyman Alpha Reference Sample: II. HST Imaging Results, Integrated Properties And Trends", submitted to APJ
 Hayes+ (2013), "Lyman Alpha Reference Sample: Extended Lyman Alpha Halos Produced At Low Dust Content", APJL, 765:L27, 2013
 Magdis+ (2011), "GOODS-Herschel: Gas-to-dust Mass Ratios and CO-to-H $_2$ Conversion Factors in Normal and Starbursting Galaxies at High-z", APJL, 740:L15, 2011
 Pardy+ (2014), "Lyman Alpha Reference Sample: III. Properties of the Neutral ISM from GBT and VLA Observations", submitted to APJ
 Östlin+ (2009), "Lyman Alpha Morphology of Local Starburst Galaxies: Release of Calibrated Images", AJ, 138:923-940, 2009